THE JOURNAL OF PHYSICAL CHEMISTRY B

Article

pubs.acs.org/JPCB

Kinetics of the Terminal Electron Transfer Step in Cytochrome *c* Oxidase

Varomyalin Tipmanee[†,‡] and Jochen Blumberger*[,‡]

[†]Department of Chemistry, University of Cambridge, Lensfield Road, Cambridge CB2 1EW, United Kingdom

[‡]Department of Physics and Astronomy, University College London, London WC1E 6BT, United Kingdom

Supporting Information

ABSTRACT: Cytochrome *c* oxidase (cco) catalyzes the oxygen reduction reaction in most aerobically respiring organisms. Decades of research have uncovered many aspects relating to structure and function of this enzyme. However, the origin of the unusually fast terminal electron transfer step from heme a to heme a_3 in cco has been the subject of intense discussions over recent years. Yet, no satisfactory consensus has been achieved. Carrying out large-scale molecular dynamics simulation of the protein embedded in a solvated membrane, we obtain a reorganization free energy $\lambda = 0.57$ eV. Evaluation of the quantized single-mode rate equation using the experimental rate and the computed reorganization free energy gives a value of 1.5 meV for the average electronic coupling (H_{ab}) between heme a and heme a_3. Thus, according to our calculations, the nanosecond electron transfer (ET) is due to a small but significant activation barrier ($\Delta G^{\ddagger} = 0.12$ eV) in combination with effective electronic coupling between the two cofactors. The activation free energy is caused predominantly by collective reorganization of protein residues. We show that our results are consistent with the weak temperature dependence observed in experiment if one allows for very minor variations in the donor–acceptor distance as the temperature changes.

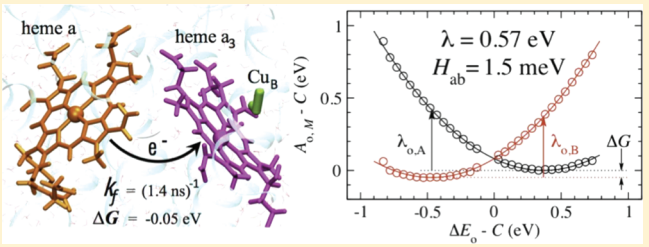

1. INTRODUCTION

Cytochrome *c* oxidase (cco) or complex IV of the respiratory chain is a truly remarkable enzyme. It catalyzes the four-electron reduction of molecular oxygen into water and couples the free energy released by this reaction to proton pumping across the mitochondrial membrane, see Figure 1. The proton gradient generated by cco is used by the neighboring enzyme adenosinetriphosphatase (ATPase) for adenosine 5′-triphosphate (ATP) production. Because of its significance for all aerobically respiring organisms, cco has been the subject of intense research for several decades. Crystal structures,[1,2] mutation experiments,[3,4] kinetic[3] and spectroscopic[5] measurements, theoretical modeling,[6−8] and molecular simulations[9−11] have given valuable insight into many key features of cco such as the nature of intermediates and conserved residues, electron- and proton-transfer pathways, and pumping mechanism. However, some important properties of cco are still poorly understood and remain a central objective of contemporary biochemical research.

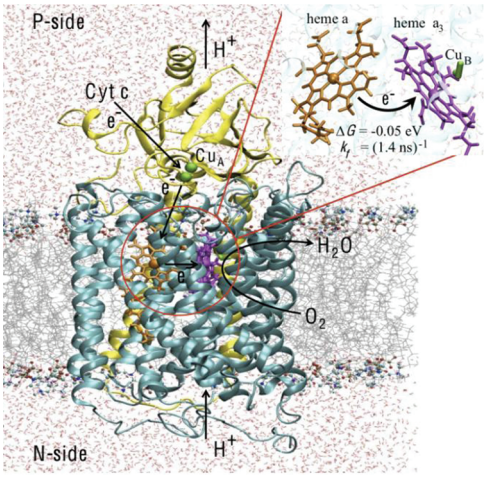

Figure 1. Cytochrome *c* oxidase subunit 1 (green) and 2 (yellow) embedded in a model lipid bilayer (gray) and solvated with an aqueous ionic solution (red, ions omitted). The inset shows the heme a to heme a_3 ET reaction simulated in this work.

One of the issues that has been much debated in recent years is the kinetics of the terminal electron transfer (ET) step from heme a to heme a_3. Using optical spectroscopy, Verkhovsky et al.[12] reported the first signatures of an ultrafast nanosecond tunneling rate for this reaction, which was later confirmed by Pilet et al.[13] and Jasaitis et al.[14] for cco and cytochrome bo_3.[15] This rate is unusual in the sense that it is at least 3 orders of magnitude faster than typical ET times in proteins[16,17] exceeded only by the ps charge separation event occurring in photosynthetic reaction centers. It was argued that the fast heme a to a_3 tunneling rate could help increase the chances of

Received: July 22, 2011
Revised: November 7, 2011
Published: January 13, 2012

dx.doi.org/10.1021/jp209175j | J. Phys. Chem. B 2012, 116, 1876–1883

trapping O_2 since oxygen only binds to reduced heme a_3.[13] In this case, the high rate for heme a to a_3 tunneling should be advantageous in particular under conditions where oxygen is a limited resource, for example, at low atmospheric pressure.

Biological ET reactions are often interpreted in terms of semiclassical Marcus theory[18] relating the ET rate (k_c) to the three parameters electronic coupling (H_{ab}), reorganization free energy (λ), and driving force (ΔG)

$$k_c = \frac{2\pi}{\hbar}|H_{ab}|^2(4\pi\lambda k_B T)^{-1/2}\exp\left(-\frac{(\lambda+\Delta G)^2}{4\lambda k_B T}\right) \quad (1)$$

For heme a to a_3 ET, the driving force is small ($\Delta G \approx -0.05$ eV).[14] Thus, in the Marcus picture, the high ET rate of this reaction is due to large electronic coupling between the cofactors or a small activation free energy, $\Delta G^{\ddagger} = (\lambda + \Delta G)^2/4\lambda$, that is, small λ, or a favorable combination of both parameters. These possible alternatives for the explanation of the nanosecond tunneling rate have divided the community for several years. Early empirical predictions based on the Moser-Dutton expression for electronic coupling were consistent with a nanosecond rate if a reorganization free energy as high as 0.7 eV was assumed.[16,19] The activation free energy corresponding to this value ($\Delta G^{\ddagger} = 0.15$ eV at 300 K) is in apparent contrast with the results of temperature-dependent rate measurements, which show that the rate remains almost unchanged in the temperature range 277−308 K.[14] Semiempirical calculations of electronic couplings[20] and recent molecular dynamics estimates of reorganization free energy[21] have further supported the notion that heme a to a_3 tunneling is almost activationless and should be described by a reorganization free energy as low as 0.2 eV ($\Delta G^{\ddagger} = 0.03$ eV). Such low values are highly unusual for thermal electron transfer in proteins and are surprising indeed if one bears in mind that the reorganization energy of only two porphyrins makes already a contribution of about 0.1 eV.[22−25]

Motivated by this controversy, we have carried out large-scale molecular dynamics simulation of cco embedded in a membrane and solvated with explicit water. Calculating the reorganization free energy in a most realistic way by estimating the outer-sphere contribution with a validated electronically polarizable force field and the inner-sphere contribution by density functional theory (DFT) calculations, we obtain a value $\lambda = 0.57$ eV corresponding to a small but significant activation barrier for heme a to a_3 ET ($\Delta G^{\ddagger} = 0.12$ eV). We show that our results can quantitatively account for the weak temperature dependence of the tunneling rate if one allows for very minor variations in the electronic coupling matrix element as the temperature varies, which is an important issue that has not been considered in previous interpretations.

2. COMPUTATIONAL METHODOLOGY

2.1. Theory. The reorganization free energy for heme a to heme a_3 ET in cco is calculated according to a quantum mechanics plus molecular mechanics (QM + MM) approach that was described in detail in previous publications.[25,26] The total reorganization free energy λ is divided into the contribution of the heme a and heme a_3 cofactors and their axial ligands, λ_i (subscript i for inner sphere), and the contributions of the protein, solvent, and membrane, λ_o (subscript o for outer sphere)

$$\lambda = \lambda_i + \lambda_o \quad (2)$$

The assumption of additivity of reorganization free energy as implied by eq 2 has been tested previously by QM/MM calculations on cytochrome *c* and was found to give sufficiently accurate results.[26] In previous work, we also benchmarked the QM + MM scheme against Born−Oppenheimer density functional molecular dynamics (all QM) for oxidation of aqueous $Ru(bpy)_3^{2+}$ (see Table 3 of the Supporting Information of ref 27). The difference in reorganization free energy obtained for the two schemes was 0.04 eV. We expect a similarly small difference for the heme a to a_3 ET if one were able to do density functional molecular dynamics (MD) on the whole protein.

The inner-sphere reorganization energy was calculated at the DFT level of theory for gas-phase models of the heme a and heme a_3 cofactors (see section 2.2 for details). The outer-sphere contribution is obtained from the thermal averages of the vertical energy gap $\Delta E_o = E_{B,o} - E_{A,o}$ in the initial (A) and final diabatic states (B)

$$\lambda_o = 1/2(\langle \Delta E_o \rangle_A - \langle \Delta E_o \rangle_B) \quad (3)$$

where in state A the excess electron is localized on heme a (Fe^{2+}−heme a−Fe^{3+}−heme a_3) and in state B on heme a_3 (Fe^{3+}−heme a−Fe^{2+}−heme a_3). The outer-sphere energy $E_{M,o}$ is the potential energy of the total system in state M (M = A, B) minus the potential energy of the atoms that comprise the inner-sphere region. Thus, the classical inner-sphere contribution is not included in eq 3 as it is obtained at the QM level. In this way, double counting of the inner-sphere contribution is avoided. The validity of the linear response (or Gaussian) assumption underlying eq 3 was investigated by calculation of the reorganization free energy from the variance of the energy gap in states A and B

$$\lambda_o' = (\langle \delta\Delta E_o^2 \rangle_A + \langle \delta\Delta E_o^2 \rangle_B)/(4k_B T) \quad (4)$$

and by explicit construction of the ET free energy curves

$$A_{o,M} = -k_B T \ln p_M(\Delta E_o) \quad (5)$$

where p_M is the probability distribution of the energy gap in states M = A, B. In the limit of linear response, $\lambda_o = \lambda_o' = \lambda_{o,M}$, where $\lambda_{o,M}$ is the reorganization free energy obtained from the diabatic free energy curves of eq 5. The thermal averages in eq 3 are obtained from molecular dynamics (MD) simulation as detailed in section 2.3.

The temperature dependence of the experimental ET rates is analyzed in terms of the quantized single-mode rate equation[28]

$$k_q' = \frac{2\pi}{\hbar}|H_{ab}|^2 FC' \quad (6a)$$

$$FC'(\omega) = \frac{1}{\hbar\omega}\left(n+\frac{1}{n}\right)^{P/2} I_P(2S(n(n+1))^{1/2}) \exp(-S(2n+1)) \quad (6b)$$

which reduces to the semiclassical rate eq 1 in the limit $\hbar\omega \to 0$. In eq 6b, $S = \lambda/\hbar\omega$, $P = -\Delta G/\hbar\omega$, $n = 1/[\exp(\hbar\omega/k_B T) - 1]$, and I_P is the modified Bessel function of the first kind of order P. The effective mode ω is obtained by matching the single-mode Franck−Condon factor (FC′) on the right-hand side of eq 6b with the full FC factor that includes all frequencies coupling to ET[29]

$$k_q = \frac{2\pi}{\hbar}|H_{ab}|^2 FC \quad (7a)$$

dx.doi.org/10.1021/jp209175j | J. Phys. Chem. B 2012, 116, 1876−1883

$$\mathrm{FC} = \frac{\beta}{2\pi}\int_{-\infty}^{+\infty} \mathrm{d}R \exp\left[-(\beta/2 + i\beta R)\Delta G - \frac{2}{\pi\hbar}\int_0^{\infty} \mathrm{d}\omega \frac{J(\omega)}{\omega^2}\frac{\cosh(\beta\hbar\omega/2) - \cosh(iR\beta\hbar\omega)}{\sinh(\beta\hbar\omega/2)}\right] \quad (7b)$$

The spectral density function $J(\omega)$ on the right-hand side of eq 7b is given by

$$J(\omega) = \frac{\beta\omega}{2}\int_0^{\infty} \mathrm{d}t\langle\delta\Delta E(0)\delta\Delta E(t)\rangle_{\mathrm{A}}\cos\omega t \quad (8)$$

where $\beta = 1/k_{\mathrm{B}}T$ in eqs 8 and 7b. The time correlation function of the energy gap, $\langle\delta\Delta E(0)\delta\Delta E(t)\rangle_{\mathrm{A}}$, where $\delta\Delta E = \Delta E - \langle\Delta E\rangle_{\mathrm{A}}$, is obtained from MD simulation of the full system including protein, membrane, and solvent. The protocol of this simulation is the same as the one reported previously for cytochrome proteins.[25]

2.2. Density Functional Calculations. The inner-sphere reorganization energy was calculated according to the usual four-point scheme[25,26] (eq 3 in ref 25) using the PBE exchange correlation functional[30] and the 6-31+G(d,p) basis set. Heme a was modeled as Fe(porphin)(methylimidazole)$_2$ and heme a_3 as Fe(porphin)(methylimidazole)(H_2O). The experimental spin ground state (low spin for Fe^{2+} and Fe^{3+}–heme a and high spin for Fe^{2+} and Fe^{3+}–heme a_3) could be reproduced with the PBE functional. Moreover, we found that the reorganization energy is quite robust with respect to the exchange correlation functional used varying by less than 0.05 eV for PBE and B3LYP[31,32] functionals. The Gaussian03 package was used for all DFT calculations.[33]

2.3. Molecular Dynamics Simulation of Cytochrome *c* Oxidase. *Preparation of Simulation System.* The MD simulations were carried out for a realistic extended system comprised of subunits 1 and 2 of cco embedded in a model phospholipid membrane and solvated with an ionic aqueous solution as shown in Figure 1. In a previous study, the mixed valence state resembling state E of the catalytic cycle was investigated,[21] and this state was also simulated in this work in order to allow for a consistent comparison. The initial coordinates of subunits 1 and 2 of cytochrome *c* oxidase (cco) were taken from the X-ray crystal structure (1.8 Å resolution), pdb code 1V54[2]. The excess electron is localized either on heme a or heme a_3, and the Fe atom of heme a_3 binds an axial water ligand. Cu_B is modeled in the reduced Cu^+–OH state, and Cu_A is modeled in the oxidized state. Hydrogen atoms are added using the xleap facility of the AMBER10 package.[34] All amino acids are assigned their standard protonation state at pH 7 except Glu242 and Asp364, which are protonated.[21] All histidines are singly protonated at the δ–N, except His161, His204, and His240, which are protonated at the ε-N. The tyrosine residue adjacent to Cu_B (Tyr244) is modeled protonated. All crystallographic water molecules inside the protein and near the surface are retained. In addition, four water molecules are added into the cavity above Glu242 as suggested in ref 35. The simulation system containing the protein, membrane, and solvent was prepared following closely the procedure described in refs 9, 36, and 37. The upper (P-side) and lower (N-side) phospholipid layer was generated by randomly inserting 292 pre-equilibrated 1,2-dimyristoyl-*sn*-glycero-3-phosphocholine (DMPC) molecules in an area of 90 × 90 Å^2 using PACKMOL.[38] The protein was inserted into the bilayer so that its center of mass was aligned with the center of mass of the bilayer. All DMPC molecules within 4 Å of protein atoms were then removed leaving 92 and 93 DMPC molecules in the upper and lower layer, respectively. The total charge of the system was neutralized by adding 16 Na^+ ions to the P-side and 5 Na^+ ions to the N-side of the membrane (the part of the protein within the membrane was already neutral). The protein–membrane system was solvated by adding water molecules and Na^+ and Cl^- ions to obtain a 0.1 M NaCl solution at each side of the membrane. The total number of water molecules (including crystal waters) and Na^+ and Cl^- ions are 23 202, 61, and 40, respectively.

Molecular Models. The AMBER charge parametrization of ref 39 is used for heme a, heme a_3, Cu_A, and Cu_B (see Tables 1–4 in the Supporting Information (SI)), and the charge parametrization of ref 40 is used for DMPC molecules. The equilibrium bond lengths of the cofactors and ligating residues are obtained from DFT calculations on the gas-phase models described in section 2.2. Force constants for bonding and angular terms are extracted from the Hessian computed for the minimum energy structure at the PBE/6-31G(d,p) level of theory using Seminario's algorithm. The latter is fully invariant with respect to the choice of internal coordinates.[41] The force constants for the bonding interactions between Fe and the nitrogen atoms are 227 (a, red, eq), 259 (a, red, ax), 230 (a, ox, eq), 295 (a, ox, ax), 97.5 (a_3, red, eq), 68 (a_3, red, ax), 77 (a_3, ox, eq), and 94 (a_3, ox, ax) kcal mol^{-1} Å^{-2}, where a and a_3 denote the low-spin heme a and the high-spin heme a_3 cofactors, red and ox denote reduced and oxidized state, and eq and ax denote equatorial ligands (porphyrin nitrogen atoms) and axial ligands (εN of histidine). The force constants for the bonding interaction between Fe of heme a_3 and the oxygen atom of the axial water ligand are 10 and 26 kcal mol^{-1} Å^{-2} for reduced and oxidized states, respectively. All other force constants used for the cofactors of cytochrome *c* oxidase are given in the topology file included in the SI of this article. The reorganization free energy is not sensitive to the exact value of the force constants used because the contributions from the cofactors are obtained from DFT calculations (see section 2.2). For the protein and solvent, the default force field values are taken. Simulations are carried out with the nonpolarizable AMBER99 force field[34] and TIP3P water[42] and with the electronically polarizable AMBER02 force field[34] in combination with POL3 water.[43] In the polarizable simulations, the default atomic polarizabilities are used except for the atoms of cofactors Cu_A and Cu_B and the atoms of heme a and heme a_3 that change charge during ET. These atoms are treated as nonpolarizable.

Simulation Protocol. The initial equilibration of the system was carried out with the nonpolarizable AMBER99 protein force field and TIP3P water using the NAMD program.[44] The system was energy minimized and was equilibrated in the Fe^{2+}–heme a–Fe^{3+}–heme a_3 state (initial state A) in several stages. First, the lipid tails were equilibrated for 800 ps while all other atoms of the system were fixed. The simulation was carried out in periodic boundary condition at constant volume, and the temperature was rescaled to 310 K every 1 ps. The electrostatic interactions were calculated using particle mesh Ewald summation; the cutoff for nonbonded interactions was 15 Å and the integration time step was 1 fs. Second, the protein, membrane, and aqueous solution were equilibrated for 500, 250, and 250 ps in the NPT ensemble at 310 K and 1 bar by gradually releasing harmonic restraints on the protein and

crystal water atoms with force constants of 10, 5, and 2.5 kcal mol^{-1} Å^{-2}. The pressure was controlled by the anisotropic Nose-Hoover Langevin piston method applying a constant ratio for cell fluctuations in the $x-y$ direction (in plane of the membrane). The temperature was controlled by Langevin dynamics, and the integration time step was increased to 2 fs. All hydrogen bonds were constrained using the SHAKE algorithm. During this equilibration period, water molecules were prevented from penetrating the lipid bilayer by applying a pulling force in the z direction (normal to the membrane) whenever a water molecule reached an imaginary plane in the xy direction defined by the average position of the C10 atoms of the DMPC molecules. Finally, all restraints on protein atoms were removed and were replaced by a single position restraint on the center of mass of the protein with force constant 10 kcal mol^{-1} Å^{-2}. To maintain planarity of the membrane, the center of mass of the lipid head groups in the upper and lower layer were position restrained in the z direction to +17 and −17 Å relative to the center of mass of the bilayer using a force constant of 10 kcal mol^{-1} Å^{-2}. The restraints on the protein center of mass and the lipid head groups were applied in all subsequent runs. After a final equilibration period of 1.5 ns, a production run of 3.5 ns was carried out. The simulation of the final ET state (Fe^{3+}−heme a−Fe^{2+}−heme a_3, state B) was initiated from an equilibrated structure of the initial state and was equilibrated for 1.5 ns followed by a production period of 3.5 ns. The average energy gaps $<\Delta E_o>_A$ and $<\Delta E_o>_B$ were obtained from 350 equidistantly spaced configurations along the initial and final state trajectories. For an explicit expression of ΔE_o, see eqs 6 and 7 in ref 25. The electronically polarizable simulations were carried out with the sander program of the AMBER10 simulation package.[34] The simulation for state A was initiated from an equilibrated configuration taken from the nonpolarizable simulation. All system parameters were the same or equivalent to the ones used in the nonpolarizable simulation if not mentioned otherwise. Pressure and temperature was controlled by a Berendsen thermostat, and the restraint on the center of mass of the head groups was replaced by a restraint on the C10 atom of DMPC molecules using a force constant of 10 kcal mol^{-1} Å^{-2}. The induced dipoles were propagated according to the Car−Parrinello scheme using default parameter. The nuclear dynamics was integrated with a time step of 1 fs. A total of 1.25 ns was simulated, and the last 0.6 ns of the trajectory was taken for calculation of the thermal average $<\Delta E_o>_A$. For the electronically polarizable simulation of state B, trajectories were initiated from configurations along the trajectory of state A at 0.48, 0.750, and 1.1 ns denoted by arrows in Figure 2A and were run for 1.55, 1.55, and 1.9 ns, respectively. The last 0.6 ns of these trajectories was taken for calculation of $<\Delta E_o>_B$.

3. RESULTS

The MD simulations give stable equilibrium structures with protein backbone root-mean-square deviations of 1.2 and 1.3 Å for states A and B, respectively, for the nonpolarizable force field and 1.5 and 1.5 Å, respectively, for the polarizable force field. All values are relative to the crystal structure pdb code 1V54. The membrane surface area per head group is 58.0 Å^2 and 56.9 Å^2 for nonpolarizable and polarizable force field simulations, respectively. This is close to previously reported values for the same membrane model (55.8 Å^2[40]) and in good agreement with experiment (60.6 Å^2 (ref 45) and 62.2 Å^2 (ref 46)).

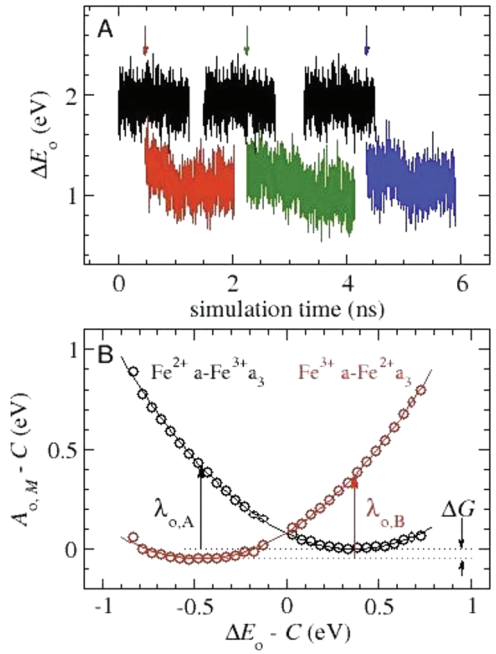

Figure 2. (A) Fluctuations of the outer-sphere vertical energy gap ΔE_o in the initial (black) and final states (red, green, blue) of cco. (B) Diabatic free energy curves of eq 5 for initial (black circles) and final states (red circles) obtained from the data shown in A and constructed as described in refs 26 and 47. Parabolic fit functions are shown in thin lines. C is a constant chosen so that the free-energy difference between the minima of the two diabatic curves is equal to the experimental free energy for ET from heme a to heme a_3. The outer-sphere reorganization free energies of the two states, $\lambda_{o,M}$ (M = A, B), is invariant with respect to the choice of this constant.

The results obtained for heme a to a_3 ET are summarized in Table 1 and Figure 2. In panel A, we show the fluctuations of the vertical energy gap ΔE_o along molecular dynamics trajectories of cco using the electronically polarizable force field. The fluctuations shown in black are for the initial state trajectory. Final state simulations are initiated from three configurations along the initial state trajectory as indicated by arrows. As one can see, the energy gap decreases in response to the change in ET state. This is due to reorganization of the system from the equilibrium structure of the initial state to the equilibrium structure of the final state. After about 1 ns, the energy gap stabilizes and fluctuates around an equilibrium value. The following 0.6 ns of dynamics is used for calculation of the thermal averages of ΔE_o, which are inserted into eqs 3 and 4 to obtain reorganization free energies. Taking the average over the three separate runs, we obtain λ_o = 0.43 eV and λ_o' = 0.42 eV, respectively. The values for each separate run differ by not more than 0.03 eV (see Table 1), which can be regarded as a statistical error estimate.

The sensitivity of outer-sphere reorganization free energy on the molecular parameter used should be discussed in more detail. In our model, the cofactors are treated as nonpolarizable atoms and the remaining system as electronically polarizable atoms. This choice was based on the following considerations: (a) It is essential to model the outer-sphere medium electronically polarizable (as repeatedly pointed out in the literature, see e.g., refs 25, 26, and 48−51). For heme a to heme a_3 ET, the outer-sphere reorganization free energy obtained with the nonpolarizable AMBER99 force field appears to be too large overestimating the value obtained with the polarizable

dx.doi.org/10.1021/jp209175j | J. Phys. Chem. B 2012, 116, 1876−1883

Table 1. Summary of the Results of Molecular Dynamics Simulation of Heme a to a_3 ET in Cytochrome *c* Oxidase Using Nonpolarizable and Polarizable Force Fields

	nonpolarizable	polarizable 1	polarizable 2	polarizable 3	average 1−3
$\langle\Delta E_o\rangle_A$ (eV)	2.37 ± 0.02	1.93 ± 0.01	1.93 ± 0.01	1.93 ± 0.01	
$\langle\Delta E_o\rangle_B$ (eV)	1.10 ± 0.02	1.09 ± 0.02	1.10 ± 0.01	1.00 ± 0.02	
$\langle\delta\Delta E_o^2\rangle_A^{1/2}$ (eV)	0.19	0.15	0.15	0.15	
$\langle\delta\Delta E_o^2\rangle_B^{1/2}$ (eV)	0.20	0.15	0.15	0.16	
λ_o[a] (eV)	0.64	0.42	0.41	0.46	0.43
λ_o'[b] (eV)	0.75	0.42	0.40	0.43	0.42
λ_p[c](eV)		0.27	0.32	0.35	0.31
λ_w[c] (eV)		0.15	0.08	0.09	0.11
λ_m[c] (eV)		0.00	0.01	0.02	0.01
λ_i[d] (eV)	0.14	0.14	0.14	0.14	0.14
λ[e] (eV)	0.78	0.56	0.55	0.60	0.57

[a]Equation 3. [b]Equation 4. [c]Reorganization free energy due to protein (λ_p), water + ions + periodic images (λ_w), and membrane (λ_m); $\lambda_o = \lambda_p + \lambda_w + \lambda_m$. [d]Total inner-sphere reorganization energy (λ_i) due to heme a and heme a_3 modeled as Fe(porphin)(methylimidazole)$_2$ (0.02 eV) and Fe(porphin)(methylimidazole)(H_2O) (0.12 eV), respectively. [e]Equation 2.

AMBER02 force field by 34%. The results remain insensitive (by less than 0.01 eV) with regard to the treatment of the Cu_A and Cu_B cofactors (nonpolarizable or polarizable) indicating that the reduction in reorganization free energy upon inclusion of electronic polarization is a collective effect of the outer-sphere medium. Moreover, we found that the results are only weakly dependent on the precise values used for the atomic polarizabilities (see Table 5 in the SI). Scaling the latter uniformly for all atoms by a factor of 1.5 (0.5), λ_o decreases (increases) by 0.03 eV only. This is reassuring in view of the tendency of the POL3 model to slightly underestimate electronic polarization effects.[52] (b) For the purpose of computing reorganization free energies, we find that it is not essential to treat the cofactor atoms of heme a and heme a_3 polarizable. (This may not be the case for other properties such as reduction potentials.) This is because the outer-sphere reorganization depends only weakly on the details of the modeling of the excess charge distribution in the hemes. We have shown this in previous work for small cytochromes,[26] and we also illustrate this here for heme a to a_3 ET in cytochrome *c* oxidase. To this end we compare two extreme cases, one where the excess electron is delocalized over all cofactor atoms as obtained from the RESP charge model (results summarized in Table 1) and the other where the excess electron is fully localized on the Fe atom of heme a in the initial state and on the Fe atom of heme a_3 in the final state (results summarized in Table 6 in the SI). In this latter charge model, the initial state is modeled by the RESP charges as before, but in the final state only the two Fe atoms change charge (by +1*e* for Fe(heme a) and −1*e* for Fe(heme a_3) leaving the charges on all other atoms unchanged. As one can see from Table 1 (main text) and Table 6 (SI), the difference in outer-sphere reorganization free energy for these two extreme cases is only 0.05 eV. (c) In previous work, we have shown that the same modeling approach (nonpolarizable solute in a polarizable environment) gives good to excellent predictions for outer-sphere reorganization free energy for oxidation of and ET between aqueous ions[27,53,54] (error ≤ 0.1 eV with respect to experiment) and cofactors bound to small proteins.[25,26]

The close correspondence of λ_o and λ_o' already indicates that the linear response assumption of Marcus theory is an excellent approximation for heme a to a_3 ET. In Figure 2B, we show the diabatic free energy curves of eq 5, which were constructed as described in refs 26 and 47 using the simulation data shown in black and red in Figure 2A. The minimum of the free energy curve for the initial state is aligned to zero, and the minimum of the final state is shifted to −0.05 eV in accord with the experimental driving force of this reaction.[14] The computed data (circles) fit parabolic curves very well with a correlation coefficient of 0.9997. The reorganization free energies obtained from the free-energy curves ($\lambda_{o,A}$ and $\lambda_{o,B}$) are the same and are virtually identical with the linear response estimate λ_o.

Addition of the inner-sphere reorganization energy, λ_i = 0.14 eV, to λ_o gives the total reorganization free energy λ = 0.57 eV. The latter is clearly dominated by the outer sphere. The main outer sphere medium is the protein with a contribution of 0.31 eV. The reorganization free energy of the protein can be considered as a collective effect with no single amino acid contributing more than 0.1 eV. The highest contribution is due to Ser34 located in the vicinity of heme a (70 meV). In the initial ET state, the hydroxyl group of the side chain is hydrogen bonded to a water molecule. Upon ET, the water moves away and the hydroxyl group rotates to form a hydrogen bond with the backbone carbonyl oxygen of Gly30. The contribution due to water and salt ions is small, 0.11 eV, and the contribution due to the lipid bilayer is below the statistical accuracy. Interestingly, most of the water and ion reorganization is due to the aqueous solution above and below the lipid bilayer, more than 13 Å away from the heme a and heme a_3 cofactors, with only a minor contribution from water molecules inside the protein. This suggests that solvent reorganization would be significantly higher if the membrane were not present underscoring the importance of including a membrane model in the MD simulations.

4. DISCUSSION

The reorganization free energy for heme a to a_3 ET has often been assumed to be very low (0.2 eV) in attempts to explain the weak temperature dependence observed for this reaction.[14,15,21] The situation is analyzed in detail in Figure 3, where we compare the experimental rates reported in ref 14 (circles with error bars) and the computed rates obtained according to the quantized single-mode rate equation, eq 6a for λ = 0.2 eV (triangles), and for the reorganization free energy obtained from present MD simulations, λ = 0.57 eV (plus symbols) in the temperature range 277−308 K. For both sets of computed rates, we have used $\hbar\omega$ = 44 meV (352 cm^{-1}) with the effective mode ω obtained from MD simulation as explained in the last

dx.doi.org/10.1021/jp209175j | J. Phys. Chem. B 2012, 116, 1876−1883

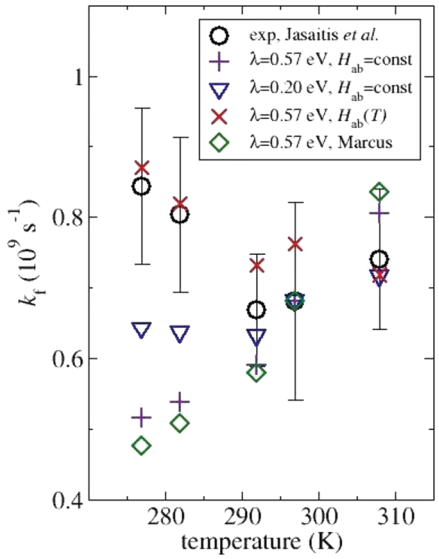

Figure 3. Rates for ET from heme a to heme a_3 in cco. Experimental values (exp) and error bars are taken from ref 14 and computed rates are obtained from eq 6a except for the data shown in green symbols which are obtained from eq 1.

paragraph of section 2.1 (eqs 6b and 7b). The coupling matrix element H_{ab} was obtained from eq 6a using the experimental rate and driving force at 297 K and the computed value for ω. For λ = 0.57 eV, this gives H_{ab} = 1.5 meV. Thus, the experimental and computed rates match at 297 K. The weak temperature dependence of ΔG as reported in ref 14 was included for these two sets of computed rates, whereas λ, H_{ab}, and ω were assumed to be temperature independent. The computed oscillator energy is somewhat smaller than what is usually assumed for biological ET reactions (about 70 meV). The rate analysis presented here is insensitive to the particular value taken for this parameter in the range 44−70 meV.

We find that for temperatures equal to or higher than 292 K the computed rates are within one error bar of the experimental value for both λ = 0.20 and 0.57 eV. Interestingly, for lower temperatures (277−292 K), the experimental rates appear to decrease with increasing temperature. The magnitude of this effect is small, however, and in the same range as the error bars. We find that neither data corresponding to λ = 0.20 or 0.57 eV can model this decrease in rate well although the agreement for the lower reorganization free energy is better.

The slight initial decrease in the rate as the temperature increases may be somewhat surprising. This tendency cannot be explained by further lowering the reorganization free energy below 0.2 eV or by increasing the effective frequency. Thus, if the single-mode rate eq 6a gives a good description for heme a to a_3 ET (which is usually assumed), the only possible explanation for the initial decrease in rate as the temperature increases is small changes in the effective electronic coupling (H_{ab}). Indeed, it is well-known that the coupling matrix element is very sensitive to small variations in the distance and orientation of donor and acceptor,[55] in this case between heme a and heme a_3, which can occur in response to changes in temperature. For illustration, if we assume exponential decay of H_{ab} with donor−acceptor distance with a decay constant β = 2 $Å^{-1}$ [55] and a minuscule increase in the distance of 0.01 Å/K as the temperature increases, we can quantitatively match the experimental data for λ = 0.57 eV and $\hbar\omega$ = 44 meV (cross symbols in Figure 3). The assumed total change in distance over the entire interval is minimal, just about 0.3 Å (0.6 Å if the lower limit β = 1 $Å^{-1}$ is considered[55]). Thus, sub-Å changes in the donor−acceptor distance are sufficient to compensate for the activation barrier corresponding to λ = 0.57 eV and to explain the weak temperature dependence of the reaction rate as observed in experiment. A similarly good match with the experimental data can be obtained if λ = 0.20 eV is used for only a very minor change in the temperature dependence of electronic coupling. Thus, our analysis implies that the reorganization free energy cannot be unequivocally determined from the temperature dependence of the rate that is shown in Figure 3 because of the uncertainties arising from the temperature dependence of electronic coupling.

Our computed value for reorganization free energy applies, strictly speaking, only to pure electron tunneling between heme a and heme a_3 in the intermediate state E of the catalytic cycle. The value may slightly change for electron tunneling in the other intermediate states, where heme a_3 is in the ferryl and Cu_B is in the cupric state. Possible variations may arise from the different ligands and the altered hydrogen bonding network between the ligands of heme a_3 and Cu_B in these states. Effects of different protonation states of the outer-sphere medium on reorganization free energy are expected to be small as we found that outer-sphere reorganization free energy is a collective effect of the protein and solvent with only small contributions arising from individual amino acids (see end of section 3).

In the following, we would like to comment on previous computational studies of this ET reaction. In a very recent computational study, a reorganization free energy of 0.2 eV was reported,[21] a value significantly smaller than reported in this work. The authors used two computational methods in their study, one based solely on molecular dynamics simulation of cytochrome *c* oxidase and the other based solely on density functional theory calculations of a large QM cluster of the active site. In their and our MD simulations, the same crystal structure of the enzyme was chosen as a starting point and the same oxidation and protonation states were chosen for the four cofactors and amino acid side chains, respectively. However, there are also important differences: (1) in our system, the protein is embedded in an explicit membrane and both sides of the membrane are solvated, whereas in ref 21 it appears that only the protein was simulated without explicit modeling of the environment; (2) in the present study, the electrostatic interactions are computed in periodic boundary conditions using Ewald summation (for MD and energy gap calculation), whereas in ref 21 electrostatic interactions were truncated at a cutoff of 20 Å; (3) in our calculations, we used the polarizable AMBER02 force field, whereas in ref 21 the nonpolarizabe CHARMM27 force field was used; and (4) in our calculations, the inner-sphere contribution was estimated from DFT calculations, whereas in the MD calculations of ref 21 the inner-sphere contribution appears to be obtained from the force field. Clearly, all these differences in the two setups could potentially contribute to the different results. However, there is one serious issue on which we need to further comment. If one uses the data reported in Figure 2A of ref 21 to calculate reorganization free energy according to the linear response formula $\lambda = 1/2(\langle\Delta E\rangle_A - \langle\Delta E\rangle_B)$ (which is exact for parabolic free energy curves, see, e.g., ref 26), one would obtain a value of approximately 1.5 eV. This estimate was obtained by noting that the horizontal positions of the minima of the two free energy curves are equal to $\langle\Delta E\rangle_A$ and $\langle\Delta E\rangle_B$, respectively. Thus, the curvature and the horizontal position of the minima

dx.doi.org/10.1021/jp209175j | J. Phys. Chem. B 2012, 116, 1876−1883

of the free energy curves do not appear to be consistent. As a consequence of this, the linear free energy relationship between diabatic free energy curves and energy gap, $A_B - A_A = \Delta E$, which follows from rigorous statistical mechanics[26,56] and which is valid even for nonparabolic free energy profiles (see ref 57 for such as case), is not fulfilled. The reason for this is not clear to us, and it seems that a further discussion of the differences of the two MD studies should be based on a revised analysis of the MD simulation data reported in ref 21. Interestingly, the reorganization energy that the same authors obtain on the basis of pure DFT calculations on a large QM cluster of the active site, 0.13 eV, is virtually identical with the inner-sphere reorganization energy that we report in the present work. Our analysis of the contribution of outer-sphere reorganization free energy shows that it is important to include the full system (protein + membrane + solvent) for the calculation of reorganization free energy, since this property is a long-ranged collective effect of the medium (see last paragraph of section 3). In this regard, the use of large but limited active site cluster models is likely to underestimate reorganization free energy.

Another computational study that gave a good agreement with experiment for very small reorganization energies ($\lambda = -\Delta G$) was the pathway calculation of ref 20. We and the authors of this study note, however, that the Huckel Hamiltonian used for calculation of electronic coupling is not expected to give quantitative estimates. For illustration, an increase in the coupling by only a factor of 3 would already be sufficient to compensate for an increase in reorganization free energy by 0.3 eV.

Our calculations also have implications on the validity of the Moser-Dutton ruler, which relates, surprisingly successfully, biological electron transfer rates to the donor−acceptor distance R by a single parameter termed the protein packing density ρ (at $\lambda = -\Delta G$).[58] In essence, the protein is considered as a square barrier for the tunneling electron with an effective barrier height determined by ρ. The latter is proportional to the number of atoms between donor and acceptor groups. It has been shown that the rates of a large number of biological ET reactions can be modeled to good accuracy by the empirical four-parameter tunneling expression $\log k_{ET} = 13 - (1.2 - 0.8\rho)(R - 3.6) - 3.1(\Delta G + \lambda)^2/\lambda$ (for exergonic reactions) using a single value $\rho = 0.76$.[58] Using this default value in combination with our computed reorganization free energy, the rate for heme a to a_3 tunneling is a factor of 5 too high. The deviation does not appear to be very large. This is of course because of the short donor−acceptor distance between heme a and heme a_3 (R = closest heme-to-heme edge distance = 6.9 Å[19]), which makes the rate less sensitive to the value for the packing density. Inserting the experimental rate and driving force and the computed λ in the above rate equation and solving for ρ, we obtain a value of 0.48. This smaller value is not surprising if one bears in mind that heme a to a_3 tunneling is likely to occur through space.[20] More generally, we expect that biological ET reactions between closely spaced cofactors are better described by packing densities that are nearer to 0.4−0.5 than to the default value 0.76.

Our estimate for packing density is consistent with the original definition of this parameter that identifies the closest heme-to-heme edge with the tunneling distance R. In recent work, an alternative definition has been proposed in which the distance and packing density between each individual atom−atom pair of the two cofactors are considered.[21] The rate is then obtained as an average over all individual atom-to-atom rates. Using this procedure, the authors obtained a mean packing density $\rho = 0.76$, virtually identical to the default value, and a large spread of distances in the range 7−21 Å. In combination with $\lambda = 0.2$ eV, a good agreement with the experimental rate was obtained. This good agreement for default ρ and low λ is due to the larger tunneling distances in the calculations of atom-to-atom rates relative to the closest heme-to-heme edge. Thus, the approach taken in ref 21 results effectively in a redefinition of the tunneling distance from the heme-to-heme edge to something that is closer to the Fe−Fe distance. Since packing densities, atom-to-atom tunneling distances, and rates are highly idealized concepts, we do not favor one particular method over the other.

5. CONCLUDING REMARKS

We have calculated the reorganization free energy for heme a to a_3 ET in cco and have obtained a small, but not unusually small, value of 0.57 eV. This is much lower than the values we reported previously for smaller heme proteins (0.9−1.3 eV)[25] and is a consequence of the hydrophobic environment created by the protein at short range and the membrane at long range. Thus, according to our calculations, the nanosecond ET rate in cco is a consequence of both small activation barrier (=0.12 eV) and efficient electronic coupling ($H_{ab} \approx 1.5$ meV). It would be interesting and challenging to verify this prediction by explicit computation of electronic coupling matrix elements using accurate electronic structure methods.

■ ASSOCIATED CONTENT

Supporting Information

Tables summarizing the charge parametrization of heme a, heme a_3, Cu_A, and Cu_B; a table summarizing reorganization free energies for different atomic polarizabilities; and a table summarizing energy gaps and reorganization free energy obtained from an alternative charge model for ionization. This material is available free of charge via the Internet http://pubs.acs.org.

■ AUTHOR INFORMATION

Corresponding Author

*E-mail: j.blumberger@ucl.ac.uk.

■ ACKNOWLEDGMENTS

We would like to thank Prof. Les Dutton for his suggestion to work on cytochrome *c* oxidase and Prof. Marten Vos, Prof. Marten Wikstrom and Dr. Ville Kaila for comments on this work. The Royal Thai Government is acknowledged for a PhD scholarship (V.T.) and The Royal Society for a University Research Fellowship and a research grant (J.B.). We would further like to thank the Center for Computational Chemistry, University of Cambridge, for computer time and assistance.

■ REFERENCES

(1) Iwata, S.; Ostermeier, C.; Ludwig, B.; Michel, H. *Nature* **1995**, *376*, 660−669.

(2) Tsukihara, T.; Shimokata, K.; Katayama, Y.; Shimada, H.; Muramoto, K.; Aoyoma, H.; Mochizuki, M.; Shinzawa-Itoh, K.; Yamashita, E.; Yao, M.; et al. *Proc. Natl. Acad. Sci. U.S.A.* **2003**, *100*, 15304−15309.

(3) Faxen, K.; Gilderson, G.; Adelroth, P.; Brzezinski, P. *Nature* **2005**, *437*, 286−289.

(4) Belevich, I.; Verkhovsky, M. I.; Wikstrom, M. *Nature* **2006**, *440*, 829−832.
(5) Iwaki, M.; Puustinen, A.; Wikstrom, M.; Rich, P. R. *Biochemistry* **2006**, *45*, 10873−10885.
(6) Popovic, D. M.; Stuchebrukhov, A. A. *FEBS Lett.* **2004**, *566*, 126−130.
(7) Blomberg, M. R. A.; Siegbahn, P. E. M. *J. Comput. Chem.* **2006**, *27*, 1373−1384.
(8) Kim, Y. C.; Wikstrom, M.; Hummer, G. *Proc. Natl. Acad. Sci. U.S.A.* **2009**, *106*, 13707−13712.
(9) Olkhova, E.; Hutter, M. C.; Lill, M. A.; Helms, V.; Michel, H. *Biophys. J.* **2004**, *86*, 1873−1889.
(10) Xu, J.; Voth, G. A. *Proc. Natl. Acad. Sci. U.S.A.* **2005**, *102*, 6795−6800.
(11) Olsson, M. H. M.; Warshel, A. *Proc. Natl. Acad. Sci. U.S.A.* **2006**, *103*, 6500−6505.
(12) Verkhovsky, M. I.; Jasaitis, A.; Wikstrom, M. *Biochem. Biophys. Acta, Bioenerg.* **2001**, *1506*, 143−146.
(13) Pilet, E.; Jasaitis, A.; Liebl, U.; Vos, M. H. *Proc. Natl. Acad. Sci. U.S.A.* **2004**, *101*, 16198−16203.
(14) Jasaitis, A.; Rappaport, F.; Pilet, E.; Liebl, U.; Vos, M. H. *Proc. Natl. Acad. Sci. U.S.A.* **2005**, *102*, 10882−10886.
(15) Jasaitis, A.; Johansson, M. P.; Wikstrom, M.; Vos, M. H.; Verkhovsky, M. I. *Proc. Natl. Acad. Sci. U.S.A.* **2007**, *104*, 20811−20814.
(16) Moser, C. C.; Keske, J. M.; Warncke, K.; Farid, R. S.; Dutton, P. L. *Nature* **1992**, *355*, 796−802.
(17) Gray, H. B.; Winkler, J. R. *Q. Rev. Biophys.* **2003**, *36*, 341−372.
(18) Marcus, R. A.; Sutin, N. *Biochim. Biophys. Acta* **1985**, *811*, 265−322.
(19) Moser, C. C.; Page, C. C.; Dutton, P. L. *Phil. Trans. R. Soc. B* **2006**, *361*, 1295−1305.
(20) Tan, M.-L.; Balabin, I.; Onuchic, J. N. *Biophys. J.* **2004**, *86*, 1813−1819.
(21) Kaila, V. R. I.; Johansson, M. P.; Sundholm, D.; Wikstrom, M. *Proc. Natl. Acad. Sci. U.S.A.* **2010**, *107*, 21470−21475.
(22) Sigfridsson, E.; Olsson, M.; Ryde, U. *J. Phys. Chem. B* **2001**, *105*, 5546−5552.
(23) Amashukeli, X.; Gruhn, N. E.; Lichtenberger, D. L.; Winkler, J. R.; Gray, H. B. *J. Am. Chem. Soc.* **2004**, *126*, 15566−15571.
(24) Blumberger, J.; Klein, M. L. *J. Am. Chem. Soc.* **2006**, *128*, 13854−13867.
(25) Tipmanee, V.; Oberhofer, H.; Park, M.; Kim, K. S.; Blumberger, J. *J. Am. Chem. Soc.* **2010**, *132*, 17032−17040.
(26) Blumberger, J. *Phys. Chem. Chem. Phys.* **2008**, *10*, 5651−5667.
(27) Seidel, R.; Faubel, M.; Winter, B.; Blumberger, J. *J. Am. Chem. Soc.* **2009**, *131*, 16127−16137.
(28) Jortner, J. *J. Chem. Phys.* **1976**, *64*, 4860−4867.
(29) Song, X.; Marcus, R. A. *J. Chem. Phys.* **1993**, *99*, 7768−7773.
(30) Perdew, J. P.; Burke, K.; Ernzerhof, M. *Phys. Rev. Lett.* **1996**, *77*, 3865−3868.
(31) Becke, A. *J. Chem. Phys.* **1993**, *98*, 5648−5652.
(32) Lee, C.; Yang, W.; Parr, R. *Phys. Rev. B* **1988**, *37*, 785−789.
(33) Frisch, M. J.; Trucks, G. W.; Schlegel, H. B.; Scuseria, G. E.; Robb, M. A.; Cheeseman, J. R.; Montgomery, J. A., Jr.; Vreven, T.; Kudin, K. N.; Burant, J. C.; et al. *Gaussian 03*, revision C.01; Gaussian Inc.: Wallingford, CT, 2004.
(34) Case, D. A.; Darden, T. A.; Cheatham, T.E., III; Simmerling, C. L.; Wang, J.; Duke, R. E.; Luo, R.; Crowley, M.; Walker, R. C.; Zhang, W.; et al. *AMBER 10*, University of California: San Francisco, CA, 2008.
(35) Riistama, S.; Hummer, G.; Puustinen, A.; Dyer, R. B.; Woodruff, W. H.; Wikstrom, M. *FEBS Lett.* **1997**, *414*, 275−280.
(36) Berneche, S.; Nina, M.; Roux, B. *Biophys. J.* **1998**, *75*, 1603−1618.
(37) Berneche, S.; Roux, B. *Biophys. J.* **2000**, *78*, 2900−2917.
(38) Martinez, L.; Andrade, R.; Birgin, E. G.; Martinez, J. M. *J. Comput. Chem.* **2009**, *30*, 2157−2164.
(39) Johansson, M. P.; Kaila, V. R. I.; Laakkonen, L. *J. Comput. Chem.* **2008**, *29*, 753−767.
(40) Gould, I. R.; Rosso, L. *J. Comput. Chem.* **2008**, *29*, 24−37.
(41) Seminario, J. M. *Int. J. Quantum Chem.* **1996**, *60*, 1271−1277.
(42) Jorgensen, W. L.; Chandrasekhar, J.; Madura, J. D.; Impey, R. W.; Klein, M. L. *J. Chem. Phys.* **1983**, *79*, 926−935.
(43) Caldwell, J. W.; Kollman, P. A. *J. Phys. Chem.* **1995**, *99*, 6208−6219.
(44) Phillips, J. C.; Braun, R.; Wang, W.; Gumbart, J.; Tajkhorshid, E.; Villa, E.; Chipot, C.; Skeel, R. D.; Kale, L.; Schulten, K. *J. Comput. Chem.* **2005**, *26*, 1781−1802.
(45) Kucerka, N.; Liu, Y. F.; Chu, N. J.; Petrache, H. I.; Tristram-Nagle, S. T.; Nagle, J. F. *Biophys. J.* **2005**, *88*, 2626−2637.
(46) Nagle, J. F. *Biophys. J.* **1993**, *64*, 1476−1481.
(47) Blumberger, J.; Sprik, M. *Theor. Chem. Acc.* **2006**, *115*, 113−126.
(48) Blumberger, J.; Lamoureux, G. *Mol. Phys.* **2008**, *106*, 1597−1611.
(49) Ceccarelli, M.; Marchi, M. *J. Phys. Chem. B* **2003**, *107*, 5630−5641.
(50) Ungar, L. W.; Newton, M. D.; Voth, G. A. *J. Phys. Chem. B* **1999**, *103*, 7367−7382.
(51) King, G.; Warshel, A. *J. Chem. Phys.* **1990**, *93*, 8682−8692.
(52) Ren, P.; Ponder, J. W. *J. Phys. Chem. B* **2003**, *107*, 5933−5947.
(53) Moens, J.; Seidel, R.; Geerlings, P.; Faubel, M.; Winter, B.; Blumberger, J. *J. Phys. Chem. B* **2010**, *114*, 9173−9182.
(54) Oberhofer, H.; Blumberger, J. *Angew. Chem., Int. Ed.* **2010**, *49*, 3631−3634.
(55) Smith, D. M. A.; Rosso, K. M.; Dupuis, M.; Valiev, M.; Straatsma, T. P. *J. Phys. Chem. B* **2006**, *110*, 15582−15588.
(56) Tachiya, M. *J. Phys. Chem.* **1993**, *97*, 5911−5916.
(57) Blumberger, J. *J. Am. Chem. Soc.* **2008**, *130*, 16065−16068.
(58) Moser, C. C.; Chobot, S. E.; Page, C. C.; Dutton, P. L. *Biochim. Biophys. Acta* **2008**, *1777*, 1032−1037.